JOURNAL OF VIROLOGY, July 2001, p. 6115–6120 Vol. 75, No. 13
0022-538X/01/$04.00+0 DOI: 10.1128/JVI.75.13.6115–6120.2001

Axonal Damage Is T Cell Mediated and Occurs Concomitantly with Demyelination in Mice Infected with a Neurotropic Coronavirus

AJAI A. DANDEKAR,[1] GREGORY F. WU,[2] LECIA PEWE,[3] AND STANLEY PERLMAN[1,2,3,4]*

Interdisciplinary Programs in Immunology[1] and Neuroscience[2] and Departments of Pediatrics[3] and Microbiology,[4] University of Iowa, Iowa City, Iowa 52242

Received 10 January 2001/Accepted 28 March 2001

Mice infected with mouse hepatitis virus (MHV) strain JHM develop primary demyelination. Herein we show that axonal damage occurred in areas of demyelination and also in adjacent areas devoid of myelin damage. Immunodeficient MHV-infected RAG1−/− mice (mice defective in recombinase activating gene 1 expression) do not develop demyelination unless they receive splenocytes from a mouse previously immunized against MHV (G. F. Wu, A. Dandekar, L. Pewe, and S. Perlman, J. Immunol. 165:2278–2286, 2000). In the present study, we show that adoptive transfer of T cells was also required for the majority of the axonal injury observed in these animals. Both demyelination and axonal damage were apparent by 7 days posttransfer. Recent data suggest that axonal injury is a major factor in the long-term disability observed in patients with multiple sclerosis. Our data demonstrate that immune system-mediated damage to axons is also a common feature in mice with MHV-induced demyelination. Remarkably, there appeared to be a minimal, if any, interval of time between the appearance of demyelination and that of axonal injury.

The hallmark of multiple sclerosis (MS) is the existence of multifocal demyelinating plaques within the central nervous system (CNS) (15, 23). Although oligodendrocytes, the myelin-producing cells of the CNS, and/or myelin sheaths appear to be targets of immune system-mediated destruction in MS, recent evidence demonstrating that axonal damage also occurs has renewed interest in the neuronal correlates of CNS demyelination. Axonal damage in the CNSs of patients with MS was demonstrated using immunohistochemical staining for amyloid precursor protein (5) or nonphosphorylated neurofilament H (NF) (25) and is likely to be a major component of the long-term disability observed in this disease. Axonal damage was observed most abundantly in areas of active demyelination but has also been detected in the white matter adjacent to areas of demyelination and in normal-appearing white matter (3, 5, 11, 25). In other studies, a decrease in the amount of the neuron-specific compound *N*-acetylaspartate in areas of demyelination was demonstrated by using magnetic resonance spectroscopy imaging (1). *N*-acetylaspartate was also decreased in normal-appearing white matter, possibly because axons were damaged as they crossed a site of demyelination or inflammation (4).

Axonal damage has been documented in rats with chronic active experimental autoimmune encephalomyelitis induced by immunization with myelin-oligodendrocyte glycoprotein (11) and in guinea pigs with chronic experimental autoimmune encephalomyelitis (17). Axonal loss, confined primarily to medium and large myelinated fibers, has also been demonstrated in mice with chronic demyelination induced by Theiler's murine encephalomyelitis virus (14, 19). Axonal loss correlated with neurological dysfunction and occurred relatively late in the disease course, suggesting that only demyelinated axons were damaged during disease progression.

Rodents infected with mouse hepatitis virus (MHV) strain JHM (MHV-JHM) develop acute and chronic demyelinating diseases (10, 12, 21). Although in this model demyelination is primary with axons mostly spared, infrequent axonal injury at sites of demyelination has also been noted (2, 22). The mechanism of axonal damage was not examined in any of these prior studies. Inoculation of immunocompetent C57Bl/6 (B6) mice with a variant of MHV-JHM with diminished tropism for neurons, strain 2.2-V-1, resulted in the appearance of demyelination and hind limb paresis at approximately 12 to 15 days postinoculation (p.i.) (6, 7). However, 6-week-old severe combined immunodeficiency or RAG1−/− mice did not develop demyelination after infection with 2.2-V-1 (9, 28). Demyelination and clinical disease developed in these mice 7 to 8 days after adoptive transfer of splenocytes from B6 mice previously immunized with MHV.

The studies described above suggest that axonal damage occurs early in the process of autoimmune or virus-induced demyelination, is immune mediated, and is a key factor in the neurological disease that develops in the human or animal host. Although extensive infiltration of lymphocytes and macrophages into the spinal cord is a consistent feature of the demyelinating lesions in all of these models, little is known about the relative importance of T lymphocytes and other cells in this process. Furthermore, the precise relationship between the onset of demyelination and appearance of axonal damage has not been well established. In this study, the adoptive transfer model of MHV-induced demyelination was used to address these issues, since the rapid onset of disease observed in this model makes it uniquely suited to analyze the early stages of axonal damage.

* Corresponding author. Mailing address: Department of Pediatrics, 2042 Medical Laboratories, University of Iowa, Iowa City, IA 52242. Phone: (319) 335-8549. Fax: (319) 335-8991. E-mail: Stanley-Perlman@uiowa.edu.

MATERIALS AND METHODS

Virus. The neuroattenuated variant of MHV-JHM, 2.2-V-1 (7), was generously provided by J. Fleming (University of Wisconsin, Madison).

Animals. Pathogen-free B6 mice were obtained from the National Cancer Institute (Bethesda, Md.). RAG1−/− mice were obtained from Jackson Laboratory (Bar Harbor, Maine). No mature B or T cells were detected in these mice by fluorescence-activated cell sorter analysis using antibodies specific for CD45R/B220, CD4, and CD8 antigens.

Animal model. B6 or RAG1−/− mice were infected with 10^3 PFU of 2.2-V-1 by intracranial injection (26). Adoptive transfer of splenocytes from B6 mice immunized intraperitoneally with wild-type MHV-JHM to infected RAG1−/− mice was performed as previously described (28). Wild-type MHV-JHM was used for immunization to maximize the anti-MHV immune response in donor animals. A total of 34 2.2-V-1-infected RAG1−/− mice were used in these experiments. Of these 34 mice, 10 did not receive any transferred cells, 16 received splenocytes treated with complement alone, and 8 received splenocytes depleted of both CD4 and CD8 T cells. No infectious virus could be detected by plaque assay in the transferred cells (28).

Antibodies. Monoclonal antibodies (MAbs) SMI-32 and SMI-99 (Sternberger Monoclonal Antibodies, Baltimore, Md.) were used to label nonphosphorylated NF and myelin basic protein (MBP), respectively. Rat anti-macrophage MAb (F4/80; Serotec, Oxford, England) and MAb to MHV-JHM nucleocapsid (N) protein (5B188.2; kindly provided by M. Buchmeier, The Scripps Research Institute) were used for immunohistochemical labeling of macrophages or microglia and virus antigen, respectively.

Histology. After perfusion with phosphate-buffered saline, brains and spinal cords were fixed in 10% normal buffered formalin in Histochoice fixative (Amresco, Solon, Ohio) or in zinc formaldehyde (Labsco, Louisville, Ky.). For examination of myelin and cell morphology, 8-μm-thick sections were stained with luxol fast blue.

Immunofluorescence assay. The distribution of nonphosphorylated NF or myelin was determined as follows. Sections (8 μm thick) from samples fixed with Histochoice or zinc formaldehyde were permeabilized with 0.1% Triton X-100, blocked with CAS BLOCK (Zymed Laboratories, San Francisco, Calif.), and incubated with primary antibody (SMI-32 diluted 1:5,000 to 1:10,000 or SMI-99 diluted 1:1,000 in 1% normal goat serum) overnight at 4°C. After the sections were washed, they were incubated with fluorescein isothiocyanate-conjugated goat anti-mouse immunoglobulin G antibody diluted 1:100 (ICN/Cappel, Aurora, Ohio) for 1 h at room temperature. No staining was present in the absence of primary antibody (data not shown).

Immunohistochemistry. Sections were incubated with F4/80 (diluted 1:200) or 5B188.2 (diluted 1:2,000) overnight at 4°C. After the sections were washed, they were incubated with biotinylated goat anti-rat antibody (F4/80) (1:200) or biotinylated goat anti-mouse antibody (5B188.2) (Jackson Immunoresearch Labs, West Grove, Pa.) (1:100) for 1 h at room temperature. Following washing, avidin-horseradish peroxidase (Jackson Immunoresearch Labs) (1:1,000) was applied for 1 h. The final substrate utilized for the staining reaction was 3,3′-diaminobenzidine (Sigma, St. Louis, Mo.). After development, sections were counterstained with hematoxylin.

Quantification of axonal damage. (i) Method 1. Spinal cord sections were examined using a Zeiss LSM510 confocal microscope. Quantification of axonal damage was performed as follows. Spinal cords were prepared and stained with antibody to nonphosphorylated NF. Using Vtrace software (Image Analysis Facility, University of Iowa), images from the white matter of an entire midsagittal section were digitized and analyzed. Damaged axons were identified as accumulations of NF in the white matter, and the number of pixels above the background level was recorded. Sections were analyzed in a blind fashion by two observers. A background level of staining was identified for each section visually using an area of white matter devoid of any SMI-32 immunoreactivity. The percentage of SMI-32-positive pixels per area of white matter in each section was determined by dividing the number of pixels above the threshold level in an average of 48 (range, 14 to 107) separate fields (magnification of ×20) by the total area of white matter.

(ii) Method 2. To compare the amount of axonal damage in demyelinated and normally myelinated areas, the number of SMI-32-immunoreactive axons per microscope field at a magnification of ×20 was determined using a Leitz DMRB microscope with a fluorescence attachment. Twelve fields (four in areas of demyelination, four in adjacent areas, and four in normal-appearing white matter) were examined per spinal cord.

Statistical analysis. *P* values were calculated by using Student's *t* test.

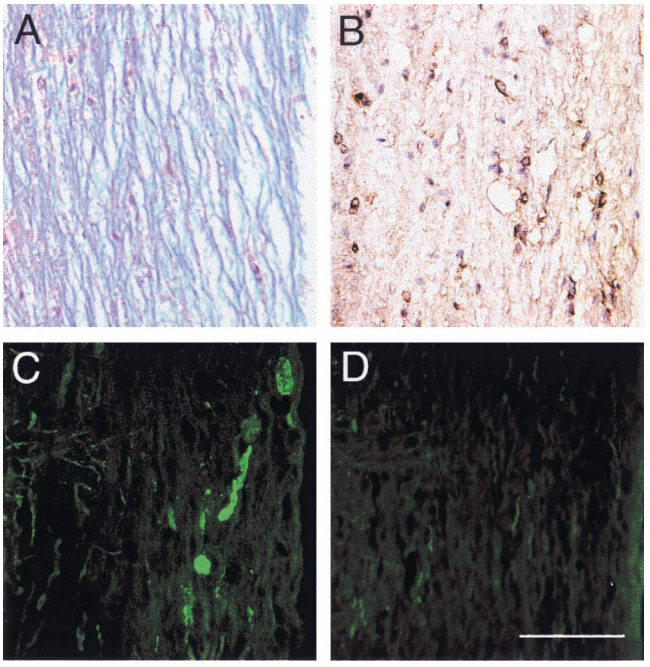

FIG. 1. Axonal damage was detected in 2.2-V-1-infected RAG1−/− mice, but not in uninfected RAG1−/− mice. Spinal cords were harvested from 2.2-V-1-infected (A to C) and uninfected (D) RAG1−/− mice. Samples were analyzed for demyelination (A), virus antigen (B), and SMI-32 immunoreactivity (C and D). Although viral antigen was abundant in the white and gray matter (B), only occasional areas of axonal debris were detected in 2.2-V-1-infected RAG1−/− mice (C). No SMI-32 immunoreactivity was detected in the white matter of uninfected mice (D). Ten 2.2-V-1-infected and four uninfected RAG1−/− mice were used in these experiments. Bar, 100 μm.

RESULTS

Axonal damage was observed following infection with 2.2-V-1. Immunocompetent B6 mice infected with the attenuated 2.2-V-1 variant of MHV-JHM develop primary demyelination within 12 days of inoculation, with relative preservation of axons (9, 26). In preliminary experiments, we analyzed these mice with demyelination for axonal damage using antibody to nonphosphorylated NF (SMI-32). In uninfected animals, nonphosphorylated NF is present in neuronal cell bodies and dendrites but is not detected in normal white matter (13). SMI-32 immunoreactivity was detected in the spinal cords of MHV-infected mice with demyelination, consistent with axonal damage (data not shown). In these immunocompetent mice, axonal damage could result from direct virus damage to axons or glial cells or could be immune mediated. To distinguish these possibilities, axonal damage was assayed in 2.2-V-1-infected RAG1−/− mice. We showed previously that 2.2-V-1-infected RAG1−/− mice do not develop demyelination in the absence of transferred splenocytes. Adoptive transfer of either MHV-specific CD4 or CD8 T cells was sufficient for the development of demyelination (27).

Initially, serial sections from naive and MHV-infected RAG1−/− mice were analyzed for axonal damage, macrophages or microglia, viral antigen, and myelin integrity. Essentially no SMI-32 immunoreactivity was detected in naive RAG1−/−mice (Fig. 1D). However, staining for nonphospho-

rylated NF was detected at low levels in the spinal cords of MHV-infected RAG1−/− mice at 10 days p.i. (Fig. 1C), although demyelination was not detected in these mice (Fig. 1A). Extensive viral replication within both the gray and white matter was present in the CNSs of these mice (Fig. 1B), showing that virus infection in the absence of T and B cells resulted in only a small amount of axonal damage.

Axonal damage was largely immune mediated. Adoptive transfer of splenocytes from immunized donors to 2.2-V-1-infected RAG1−/− mice resulted in frank demyelination by 7 days posttransfer (p.t.) (28). In these experiments, immune splenocytes were transferred to RAG1−/− mice 3 or 4 days after intracerebral inoculation with 2.2-V-1. SMI-32 immunoreactivity was markedly increased in the spinal cords of these mice, particularly in areas of demyelination (Fig. 2A and J). Several patterns of SMI-32 immunoreactivity were present in these mice (Fig. 2J), similar to those observed in the CNSs of patients with MS (25). Collections of SMI-32 staining with the appearance of debris, consistent with axonal destruction, were detected in areas of demyelination. Some axons exhibited discontinuous staining with focally enlarged caliber, consistent with degenerative changes. Ovoid bodies attached to axonal remnants, suggesting axonal transection, were also observed (e.g., inset in Fig. 2J). Nonphosphorylated NF is also present in intact demyelinated axons (25), and some of the SMI-32-immunoreactive axons appeared to be normal axons lacking myelin. Macrophages or microglia, believed to be the predominant effector cells in MHV-induced demyelination, were abundant in areas of demyelination and axonal damage (Fig. 2D). Viral antigen was also present (Fig. 2G) but at lower levels than in mice not receiving transferred splenocytes.

SMI-32 immunoreactivity was also detected in areas adjacent to demyelinating lesions (Fig. 2K). The myelin in these areas appeared relatively unaffected after staining with luxol fast blue (Fig. 2B) or with antibody to MBP (data not shown). However, even in these regions of the spinal cord, the white matter was not truly normal, since activated macrophages were detected in the general vicinity of the SMI-32-immunoreactive axons (Fig. 2E) and viral antigen was detected (Fig. 2H). This result suggested either that the inflammatory process was in its early stages in these areas or that axonal damage was a secondary effect of axonal passage through a site of demyelination or inflammation. No SMI-32 immunoreactivity was detected in some areas of normal-appearing white matter (Fig. 2L), but in these areas, virus, macrophage, and myelin disruption were not detected (Fig. 2C, F, and I).

Two approaches were taken to quantify the amount of axonal damage present in infected spinal cords. In the first approach, all the white matter was analyzed for SMI-32 immunoreactivity by confocal microscopy as described in Materials and Methods (Fig. 3A). This method facilitated comparison between 2.2-V-1-infected RAG1−/− mice that did not receive transferred cells and those that did. Transfer of immune splenocytes resulted in a significant increase in axonal damage. Since only about 10 to 15% of the white matter exhibited demyelination after adoptive transfer (27) and most axonal damage was observed in areas of myelin damage, this approach tended to blunt the differences in axonal damage observed among the various groups. Notably, only low levels of demyelination (27) or axonal damage (Fig. 3A) were detected when MHV-infected RAG1−/− mice received splenocytes depleted of both CD4 and CD8 T cells.

In a second approach, the number of damaged axons per unit area was determined in areas of demyelination and in areas of normal-appearing white matter within a single spinal cord by fluorescence microscopy (Fig. 3B). The latter were divided into areas with early signs of damage (Fig. 2B, E, H, and K) and those that appeared completely normal (Fig. 2C, F, I, and L). This analysis showed that axonal damage occurred preferentially in areas of demyelination.

Axonal damage was not detected prior to the development of demyelination. These results indicated that axonal damage was detected by day 7 to 8 p.i., at approximately the same time that demyelination was first observed. However, activated macrophages or microglia were detected at sites of viral infection in the spinal cord as early as five days p.t., although frank demyelination was not detected at this time (28). To investigate further the relationship between demyelination, macrophage or microglia infiltration and axonal damage, spinal cords were harvested from mice 4.5 days p.t., and serial sections were analyzed as described above. Macrophage infiltration into the white matter (Fig. 4B) was detected at sites of viral infection (Fig. 4C). These regions showed little evidence of myelin damage when examined by luxol fast blue staining (Fig. 4A) or by staining with antibody to MBP (data not shown). However, low levels of SMI-32 immunoreactivity were detected in these samples (Fig. 4D), suggesting that axonal injury occurred during early stages of damage to the myelin sheath. The number of damaged axons in areas of macrophage infiltration (12.8 ± 1.7 damaged axons/mm^2) and in areas lacking macrophage infiltration (2.3 ± 0.9 damaged axons/mm^2) were significantly different ($P < 0.001$) when the spinal cords of four mice were analyzed 4.5 days p.t.

DISCUSSION

These data show that axonal damage was readily detected in the spinal cords of MHV-infected mice. Axonal damage was partly T and B cell independent, since low levels were detected in infected RAG1−/− mice in the absence of adoptive transfer of immune splenocytes. However, substantial increases in SMI-32 immunoreactivity were detected following adoptive transfer, nearly coincident with the onset of demyelination. An increase in SMI-32 immunoreactivity was also detected in areas of macrophage infiltration prior to the development of overt demyelination (Fig. 4). It is likely that these were sites of incipient myelin damage and axonal injury. The results of this study are consistent with those of other studies suggesting that axonal damage occurred in the intense inflammatory milieu present at sites of demyelination but also showed for the first time that this damage occurred very early in the disease process.

We showed previously that demyelination was mediated by T cells in the adoptive transfer model (27). As shown above, axonal damage was not increased if CD4 and CD8 T cells were removed prior to adoptive transfer (Fig. 3A). Clinical disease and demyelination occurred only occasionally in mice that received splenocytes from donors not previously immunized to MHV, suggesting that MHV-specific T cells were critical for demyelination to develop (28). Our results suggest that axonal

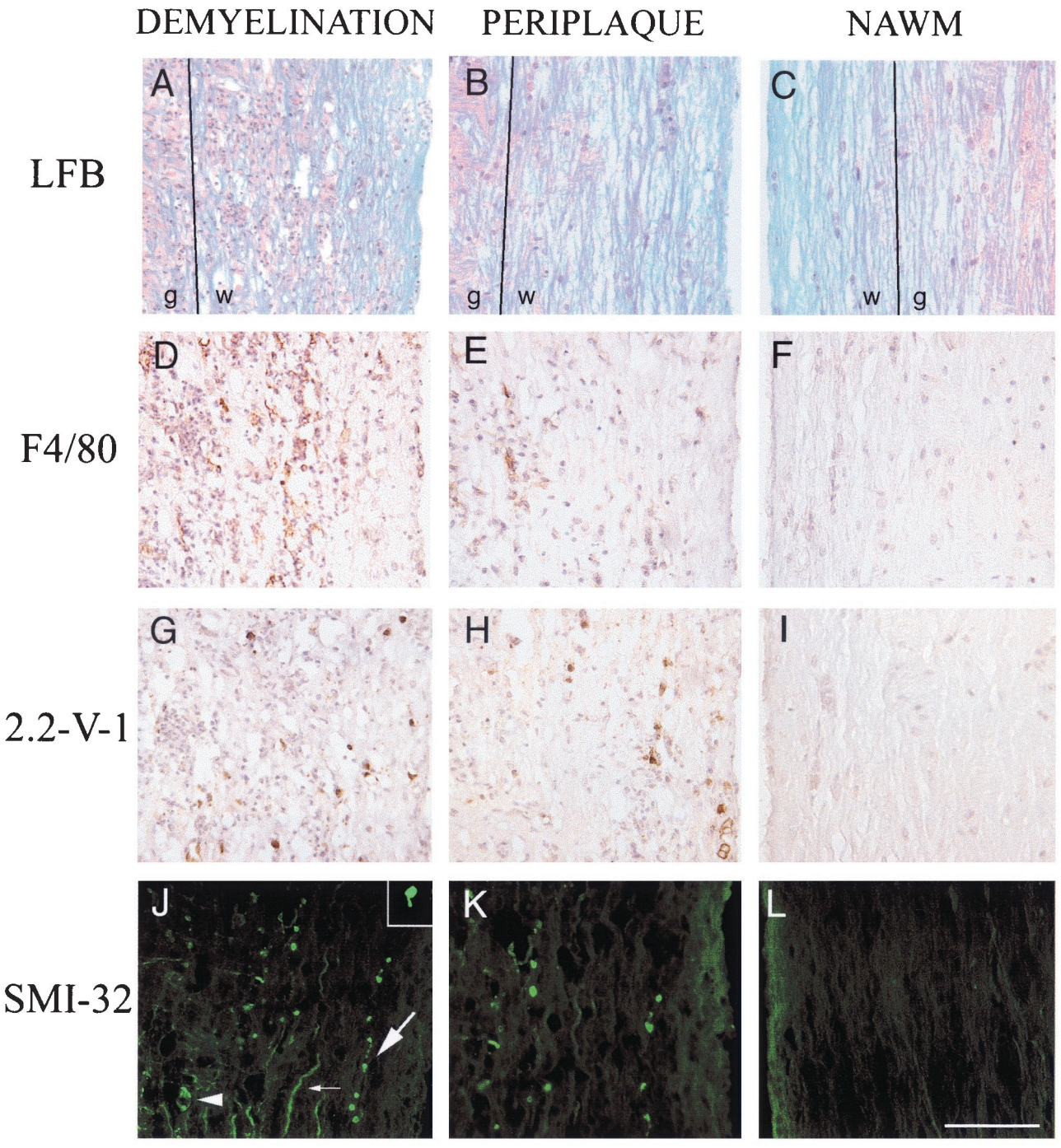

FIG. 2. Correlation of axonal damage with demyelination and macrophage infiltration. Spinal cords were harvested from RAG1−/− mice 7 days p.t. of immune splenocytes. Serial sections (8 μm thick) were analyzed for demyelination (A to C), macrophages or microglia (D to F), viral antigen (G to I), and nonphosphorylated NF (J to L). Many SMI-32-immunoreactive axons (J) were detected in areas of demyelination (A). In panel J, cellular debris (arrowhead), a degenerating axon (large arrow), and an intact demyelinated axon (small arrow) are indicated. Abundant macrophage infiltration (D) and virus antigen (G) were detected in these lesions. Examination of areas adjacent to the demyelinating lesions (periplaque) revealed relatively normal-appearing white matter (B), infiltration of macrophages (E), presence of viral antigen (H), and reduced amounts of SMI-32 immunoreactivity (K). Finally, more-distal areas of normal-appearing white matter (NAWM) (C) exhibited no macrophage infiltration (F) or viral antigen (I), with only low levels of SMI-32 immunoreactivity (L). An ovoid body associated with an axonal remnant consistent with axonal transection is shown in the inset in panel J. Eleven 2.2-V-1-infected RAG1−/− mice analyzed 7 days p.t. were used in these experiments. Abbreviations: LFB, luxol fast blue; w, white matter; g, gray matter. Bar, 100 μm.

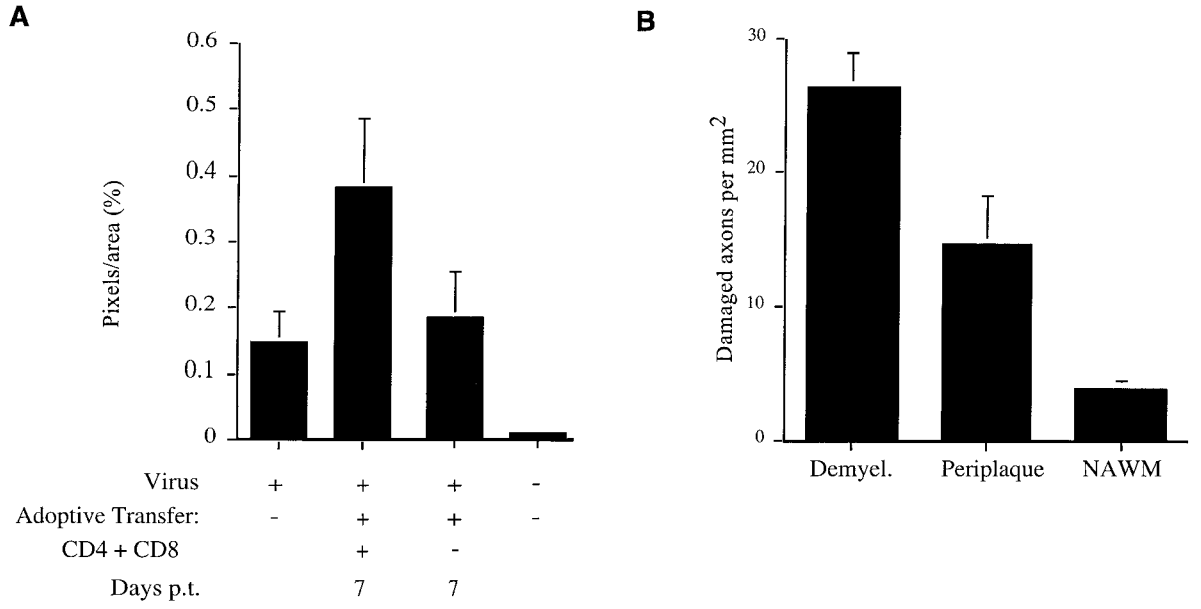

FIG. 3. Quantification of increase in SMI-32 reactivity in RAG1−/− mice following adoptive transfer. The amount of axonal damage within the white matter of spinal cords from 2.2-V-1-infected RAG1−/− mice was quantified by using two separate methods as described in Materials and Methods. (A) In the first method, the amount of SMI-32 immunoreactivity within the entire white matter of individual spinal cords was determined. Eight mice were analyzed prior to adoptive transfer (10 days p.i.). Three days p.i., eight mice received undepleted splenocyte populations, whereas an additional eight mice received splenocytes depleted of both CD4 and CD8 T cells. These mice were harvested 7 days p.t. Three uninfected mice were also analyzed. The amount of SMI-32 immunoreactivity in naive mice was significantly less than that detected in any of the virus-infected mice ($P < 0.01$). The amount of staining in mice in the absence of adoptive transfer or in mice that received splenocytes depleted of both CD4 and CD8 T cells was significantly less than in mice receiving undepleted populations ($P < 0.001$). There was no statistical difference in staining between infected mice receiving doubly depleted cells and those analyzed in the absence of adoptive transfer ($P > 0.05$). (B) In the second method, axonal damage in areas of demyelination (Demyel.), periplaque, and more-distal normal-appearing white matter (NAWM), as described in the legend to Fig. 2, was quantified by fluorescence microscopy. Spinal cords from four mice receiving adoptive transfer of undepleted splenocytes were used in these analyses. The differences between all groups are statistically significant ($P < 0.01$).

damage was also mediated by MHV-specific T cells, at least to the extent that they were required for initiating the inflammatory response that resulted in demyelination.

These results do not eliminate a role for B cells and splenic macrophages in demyelination or axonal injury but do show that they are not able to cause demyelination in the absence of T cells. It is likely that transferred macrophages are not necessary for demyelination to develop. In MHV-infected B6 mice, chemical depletion of bloodborne macrophages did not result in a decrease in demyelination (29), suggesting that microglia or perivascular macrophages were able to serve as the final effector cells of demyelination.

Our results revealed a low level of SMI-32 immunoreactivity in 2.2-V-1-infected RAG1−/− mice in the absence of adoptively transferred splenocytes. Axonal damage may be a direct consequence of viral infection of neurons or, alternatively, result from infection (and subsequent dysfunction) of glial cells, including oligodendrocytes. In mice deficient in the expression of proteolipid protein, severe axonal pathology is detected, although myelin disruption is minimal and overt demyelination is not detected (8). Damage may also be mediated by NK cells or other parts of the immune system intact in RAG1−/− mice. After adoptive transfer of immune splenocytes, axonal damage was most abundant at sites of demyelination, suggesting that the inflammatory response at sites of demyelination, and not immune-mediated clearance from neurons, was responsible for this increase in damage. In support of this, axonal damage was detected in B6 mice chronically infected with wild-type MHV-JHM (data not shown). Minimal amounts of virus were detected in the gray matter in these mice (16, 24), indicating that the process of neuronal clearance was accomplished much earlier. Furthermore, axonal damage was observed following infection of B6 mice with 2.2-V-1 (data not shown), even though replication is largely restricted to the white matter in these animals (6, 7).

SMI-32 immunoreactivity may represent reversible or irreversible axonal damage. Axonal transection is irreversible and accounted for some of the SMI-32 staining that we observed. However, both remyelinated and demyelinated axons may recover function via restoration of conduction, possibly secondary to restoration of sodium channel function (20). Axonal dysfunction resulting from impaired axonal conduction in the CNSs of mice infected with Theiler's murine encephalomyelitis virus has been reported and shown to be CD8 T cell mediated (18). In the absence of CD8 T cells, redistribution of ion channels was detected, thereby preserving neurological function, even in the presence of demyelination.

Our experiments do not address the role of axonal damage in long-term disease progression, since we analyzed mice at early times after adoptive transfer. However, they showed that axonal damage was, in large part, immune mediated in mice infected with MHV and occurs concomitantly with demyelination. This model system will be useful for determining the

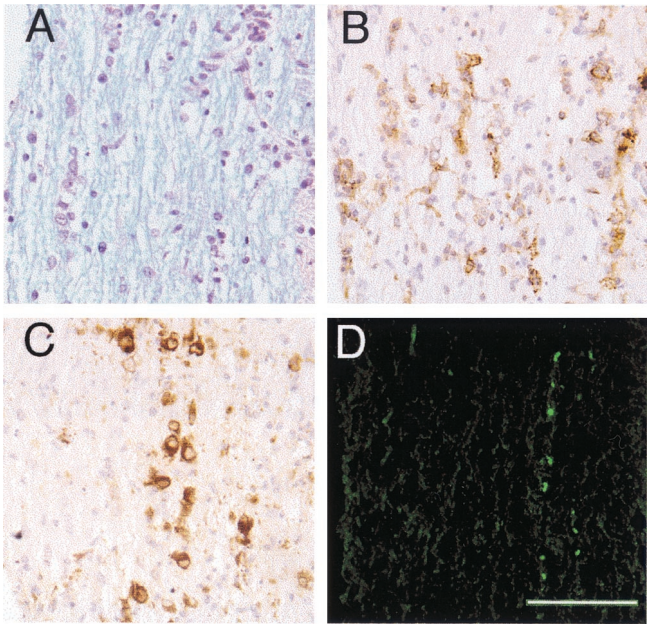

FIG. 4. Axonal damage does not precede demyelination. Serial sections (8 μm thick) from the spinal cords of 2.2-V-1-infected RAG1−/− mice harvested 4.5 days p.t. were analyzed for demyelination (A), macrophages or microglia (B), viral antigen (C), and nonphosphorylated NF (D). Examination of the spinal cords of these mice revealed no frank demyelination (A) but abundant viral antigen (C). SMI-32 immunoreactivity (D) was detected at low levels and was primarily localized to areas of macrophage or microglia infiltration (B). The data shown are representative of analyses of the spinal cords of five mice. Bar, 100 μm.

specific mechanisms responsible for axonal damage in virus-induced demyelination.

ACKNOWLEDGMENTS

Ajai A. Dandekar and Gregory F. Wu contributed equally to this work.

We thank Sonya Mehta, Image Analysis Facility, University of Iowa, for helping design methods for quantification of axonal damage.

This research was supported in part by grants from the National Institutes of Health (NS 36592 and NS 40438) and the National Multiple Sclerosis Society (RG2867-A-2). G.F.W. was supported by NRSA predoctoral fellowship MH2066-02.

REFERENCES

1. **Arnold, D. L.** 1999. Magnetic resonance spectroscopy: imaging axonal damage in MS. J. Neuroimmunol. **98:**2–6.
2. **Bailey, O., A. M. Pappenheimer, F. S. Cheever, and J. B. Daniels.** 1949. A murine virus (JHM) causing disseminated encephalomyelitis with extensive destruction of myelin. J. Exp. Med. **90:**195–212.
3. **Bitsch, A., J. Schuchardt, S. Bunkowski, T. Kuhlmann, and W. Bruck.** 2000. Acute axonal injury in multiple sclerosis. Correlation with demyelination and inflammation. Brain **123:**1174–1183.
4. **De Stefano, N., S. Narayanan, P. M. Matthews, G. S. Francis, J. P. Antel, and D. L. Arnold.** 1999. In vivo evidence for axonal dysfunction remote from focal cerebral demyelination of the type seen in multiple sclerosis. Brain **122:**1933–1939.
5. **Ferguson, B., M. Matyszak, M. Esiri, and V. Perry.** 1997. Axonal damage in acute multiple sclerosis lesions. Brain **120:**393–399.
6. **Fleming, J. O., M. D. Trousdale, J. Bradbury, S. A. Stohlman, and L. P. Weiner.** 1987. Experimental demyelination induced by coronavirus JHM (MHV-4): molecular identification of a viral determinant of paralytic disease. Microb. Pathog. **3:**9–20.
7. **Fleming, J. O., M. D. Trousdale, F. A. K. El-Zaatari, S. A. Stohlman, and L. P. Weiner.** 1986. Pathogenicity of antigenic variants of murine coronavirus JHM selected with monoclonal antibodies. J. Virol. **58:**869–875.
8. **Griffiths, I., M. Klugmann, T. Anderson, D. Yool, C. Thomson, M. H. Schwab, A. Schneider, F. Zimmermann, M. McCulloch, N. Nadon, and K. A. Nave.** 1998. Axonal swellings and degeneration in mice lacking the major proteolipid of myelin. Science **280:**1610–1613.
9. **Houtman, J. J., and J. O. Fleming.** 1996. Dissociation of demyelination and viral clearance in congenitally immunodeficient mice infected with murine coronavirus JHM. J. Neurovirol. **2:**101–110.
10. **Houtman, J. J., and J. O. Fleming.** 1996. Pathogenesis of mouse hepatitis virus-induced demyelination. J. Neurovirol. **2:**361–376.
11. **Kornek, B., M. K. Storch, R. Weissert, E. Wallstroem, A. Stefferl, T. Olsson, C. Linington, M. Schmidbauer, and H. Lassmann.** 2000. Multiple sclerosis and chronic autoimmune encephalomyelitis: a comparative quantitative study of axonal injury in active, inactive, and remyelinated lesions. Am. J. Pathol. **157:**267–276.
12. **Lane, T. E., and M. J. Buchmeier.** 1997. Murine coronavirus infection: a paradigm for virus-induced demyelinating disease. Trends Microbiol. **5:**9–14.
13. **Lee, V. M., M. J. Carden, W. W. Schlaepfer, and J. Q. Trojanowski.** 1987. Monoclonal antibodies distinguish several differentially phosphorylated states of the two largest rat neurofilament subunits (NF-H and NF-M) and demonstrate their existence in the normal nervous system of adult rats. J. Neurosci. **7:**3474–3488.
14. **McGavern, D. B., P. D. Murray, C. Rivera-Quinones, J. D. Schmelzer, P. A. Low, and M. Rodriguez.** 2000. Axonal loss results in spinal cord atrophy, electrophysiological abnormalities and neurological deficits following demyelination in a chronic inflammatory model of multiple sclerosis. Brain **123:**519–531.
15. **Noseworthy, J. H.** 1999. Progress in determining the causes and treatment of multiple sclerosis. Nature **399:**A40–A47.
16. **Perlman, S., R. Schelper, E. Bolger, and D. Ries.** 1987. Late onset, symptomatic, demyelinating encephalomyelitis in mice infected with MHV-JHM in the presence of maternal antibody. Microb. Pathog. **2:**185–194.
17. **Raine, C. S., and A. H. Cross.** 1989. Axonal dystrophy as a consequence of long-term demyelination. Lab. Investig. **60:**714–725.
18. **Rivera-Quinones, C., D. McGavern, J. Schmelzer, S. Hunter, P. Low, and M. Rodriguez.** 1998. Absence of neurological deficits following extensive demyelination in a class I-deficient murine model of multiple sclerosis. Nat. Med. **4:**187–193.
19. **Sathornsumetee, S., D. B. McGavern, D. R. Ure, and M. Rodriguez.** 2000. Quantitative ultrastructural analysis of a single spinal cord demyelinated lesion predicts total lesion load, axonal loss, and neurological dysfunction in a murine model of multiple sclerosis. Am. J. Pathol. **157:**1365–1376.
20. **Smith, K. J., and W. I. McDonald.** 1999. The pathophysiology of multiple sclerosis: the mechanisms underlying the production of symptoms and the natural history of the disease. Philos. Trans. R. Soc. Lond. B **354:**1649–1673.
21. **Stohlman, S. A., C. C. Bergmann, and S. Perlman.** 1998. Mouse hepatitis virus, p. 537–557. *In* R. Ahmed and I. Chen (ed.), Persistent viral infections. John Wiley & Sons, Ltd., New York, N.Y.
22. **Stohlman, S. A., and L. P. Weiner.** 1981. Chronic central nervous system demyelination in mice after JHM virus infection. Neurology **31:**38–44.
23. **Storch, M., and H. Lassmann.** 1997. Pathology and pathogenesis of demyelinating diseases. Curr. Opin. Neurol. **10:**186–192.
24. **Sun, N., D. Grzybicki, R. Castro, S. Murphy, and S. Perlman.** 1995. Activation of astrocytes in the spinal cord of mice chronically infected with a neurotropic coronavirus. Virology **213:**482–493.
25. **Trapp, B., J. Peterson, R. Ransohoff, R. Rudick, S. Monk, and L. Bo.** 1998. Axonal transection in the lesions of multiple sclerosis. N. Engl. J. Med. **338:**278–285.
26. **Wang, F., S. A. Stohlman, and J. O. Fleming.** 1990. Demyelination induced by murine hepatitis virus JHM strain (MHV-4) is immunologically mediated. J. Neuroimmunol. **30:**31–41.
27. **Wu, G., A. Dandekar, L. Pewe, and S. Perlman.** 2000. CD4 and CD8 T cells have redundant but not identical roles in virus-induced demyelination. J. Immunol. **165:**2278–2286.
28. **Wu, G. F., and S. Perlman.** 1999. Macrophage infiltration, but not apoptosis, is correlated with immune-mediated demyelination following murine infection with a neurotropic coronavirus. J. Virol. **73:**8771–8780.
29. **Xue, S., N. Sun, N. van Rooijen, and S. Perlman.** 1999. Depletion of blood-borne macrophages does not reduce demyelination in mice infected with a neurotropic coronavirus. J. Virol. **73:**6327–6334.